

University of Groningen

Observation of the decay $J/\psi \rightarrow e^+e^-\eta$ (1405) with η (1405) $\rightarrow \pi^0 f_0$ (980)

BESIII Collaboration; Kalantar-Nayestanaki, N.; Kappert, R.; Kavatsyuk, M.; Messchendorp, J.; Rodin, V.

Published in:
Physical Review D

DOI:
[10.1103/PhysRevD.109.012007](https://doi.org/10.1103/PhysRevD.109.012007)

IMPORTANT NOTE: You are advised to consult the publisher's version (publisher's PDF) if you wish to cite from it. Please check the document version below.

Document Version
Publisher's PDF, also known as Version of record

Publication date:
2024

[Link to publication in University of Groningen/UMCG research database](#)

Citation for published version (APA):

BESIII Collaboration, Kalantar-Nayestanaki, N., Kappert, R., Kavatsyuk, M., Messchendorp, J., & Rodin, V. (2024). Observation of the decay $J/\psi \rightarrow e^+e^-\eta$ (1405) with η (1405) $\rightarrow \pi^0 f_0$ (980). *Physical Review D*, 109(1), Article 012007. <https://doi.org/10.1103/PhysRevD.109.012007>

Copyright

Other than for strictly personal use, it is not permitted to download or to forward/distribute the text or part of it without the consent of the author(s) and/or copyright holder(s), unless the work is under an open content license (like Creative Commons).

The publication may also be distributed here under the terms of Article 25fa of the Dutch Copyright Act, indicated by the "Taverne" license. More information can be found on the University of Groningen website: <https://www.rug.nl/library/open-access/self-archiving-pure/taverne-amendment>.

Take-down policy

If you believe that this document breaches copyright please contact us providing details, and we will remove access to the work immediately and investigate your claim.

Downloaded from the University of Groningen/UMCG research database (Pure): <http://www.rug.nl/research/portal>. For technical reasons the number of authors shown on this cover page is limited to 10 maximum.

Observation of the decay $J/\psi \rightarrow e^+e^-\eta(1405)$ with $\eta(1405) \rightarrow \pi^0 f_0(980)$

M. Ablikim *et al.**
(BESIII Collaboration)

 (Received 28 July 2023; accepted 27 November 2023; published 12 January 2024)

Using a data sample of $(10087 \pm 44) \times 10^6$ J/ψ events collected by the BESIII detector in 2009, 2012, 2018 and 2019, the electromagnetic Dalitz process $J/\psi \rightarrow e^+e^-\eta(1405)$ is observed via the decay $\eta(1405) \rightarrow \pi^0 f_0(980)$, $f_0(980) \rightarrow \pi^+\pi^-$, with a significance of about 9.8σ . The branching fraction of this decay is measured to be $\mathcal{B}(J/\psi \rightarrow e^+e^-\eta(1405) \rightarrow e^+e^-\pi^0 f_0(980) \rightarrow e^+e^-\pi^0 \pi^+\pi^-) = (2.04 \pm 0.20(\text{stat}) \pm 0.08(\text{syst})) \times 10^{-7}$. The branching fraction ratio $\mathcal{B}(J/\psi \rightarrow e^+e^-\eta(1405))/\mathcal{B}(J/\psi \rightarrow \gamma\eta(1405))$ is determined to be $(1.36 \pm 0.17(\text{stat}) \pm 0.06(\text{syst})) \times 10^{-2}$. Furthermore, an e^+e^- invariant mass dependent transition form factor of $J/\psi \rightarrow e^+e^-\eta(1405)$ is presented for the first time. The obtained result provides input for different theoretical models and is valuable for the improved understanding the intrinsic structure of the $\eta(1405)$ meson.

DOI: [10.1103/PhysRevD.109.012007](https://doi.org/10.1103/PhysRevD.109.012007)

I. INTRODUCTION

The $\eta(1405)$ and $\eta(1475)$ excited isoscalar states with $J^{PC} = 0^{-+}$ were discovered in the $K\bar{K}\pi$ invariant mass distribution in $p\bar{p}$ collisions in 1967 [1]. Since then, several theoretical and experimental studies have been performed to investigate the nature of these states. They are considered to be possible candidates for pseudoscalar glueballs [2]; however their measured masses are much lower than those calculated by lattice quantum chromodynamics (QCD), which are greater than $2 \text{ GeV}/c^2$ [3–6]. Further studies from several experiments (i.e. E769 [7], MARKIII [8], L3 [9], E852 (MPS) [10], DM2 [11,12], OBELIX [13–16]) indicated that the two pseudoscalar states, $\eta(1405)$ and $\eta(1475)$, have rather different properties. The $\eta(1405)$ state has large couplings with $a_0(980)\pi$ or directly with $K\bar{K}\pi$; it can also decay into $\eta\pi^+\pi^-$, while the $\eta(1475)$ state decays mainly to $K^*\bar{K}$. Furthermore, there remain unsolved puzzles in the understanding of their production mechanism and decay properties, and it can not yet be concluded whether $\eta(1405)$ and $\eta(1475)$ are two separate states or a single state observed in different decay modes [17]. In 2012, an unusually narrow width of $f_0(980)$ resonance (10 MeV) is observed in the decay $\eta(1405) \rightarrow f_0(980)\pi^0$ [18]. This feature of the decay is explained by the TS mechanism [19]. Several theoretical papers [19–21] demonstrated that the “triangle singularity” mechanism (TSM)

could lead to the anomalously large isospin violation effect and also deform the line shapes and shift the peak positions of the $\eta(1405/1475)$. Hence, further studies of $\eta(1405/1475) \rightarrow \pi^0\pi^+\pi^-$ are imperative and will be valuable for better understanding the $\eta(1405/1475)$ puzzle and study the properties of these states.

The study of electromagnetic (EM) Dalitz decays plays an important role in the understanding of the intrinsic structure of hadrons and the interaction between photons and hadrons. In such a process, a virtual photon converts into a lepton pair, and the four-momentum transferred by the virtual photon corresponds to the invariant mass of the lepton pair. The branching fraction (BF) ratios of the EM Dalitz decays to the corresponding radiative decays of vector mesons are suppressed by 2 orders of magnitude [22–25].

The EM properties of a J/ψ to pseudoscalar transition are characterized by the EM transition form factor (TFF), which can be calculated in QCD models [26–28]. In experiments, the TFF can be directly determined by comparing the measured invariant mass spectrum of the lepton pair from the EM Dalitz decay with the quantum electrodynamics (QED) prediction for pointlike particles. The q^2 -dependent differential BF for $J/\psi \rightarrow e^+e^-\eta(1405)$, normalized to the corresponding radiative decay $J/\psi \rightarrow \gamma\eta(1405)$, is given by

$$\frac{d\mathcal{B}(J/\psi \rightarrow e^+e^-\eta(1405))}{dq^2 \mathcal{B}(J/\psi \rightarrow \gamma\eta(1405))} = |F(q^2)|^2 \times [\text{QED}(q^2)], \quad (1)$$

where the squared four-momentum transfer q^2 is equal to the square of the invariant mass of the e^+e^- pair ($M_{e^+e^-}$), $|F(q^2)|^2$ is the normalized TFF for the $J/\psi \rightarrow \eta(1405)$

*Full author list given at the end of the article.

Published by the American Physical Society under the terms of the [Creative Commons Attribution 4.0 International license](https://creativecommons.org/licenses/by/4.0/). Further distribution of this work must maintain attribution to the author(s) and the published article's title, journal citation, and DOI. Funded by SCOAP³.

transition, and QED(q^2) represents the pointlike QED result [29,30]. Measurements of the TFF may lead to a better understanding of charmonium Dalitz decays and their internal structures, and provide tests of QCD predictions.

This paper reports the first observation of the EM Dalitz decay channel of $J/\psi \rightarrow e^+e^-\pi^0\pi^+\pi^-$ with $\eta(1405)$ in the $\pi^+\pi^-\pi^0$ invariant mass ($M_{\pi^+\pi^-\pi^0}$) spectrum and the measurement of the TFF of $J/\psi \rightarrow e^+e^-\eta(1405)$. The ratio, $R = \frac{\mathcal{B}(J/\psi \rightarrow e^+e^-\eta(1405))}{\mathcal{B}(J/\psi \rightarrow \gamma\eta(1405))}$, is evaluated with inputs from a previous study of the radiative decay [18].

II. BESIII DETECTOR AND DATASET

The BESIII detector [31] records symmetric e^+e^- collisions provided by the BEPCII storage ring [32] in the center-of-mass energy range from 2.0 to 4.95 GeV, with a peak luminosity of $1 \times 10^{33} \text{ cm}^{-2} \text{ s}^{-1}$ achieved at $\sqrt{s} = 3.77 \text{ GeV}$. BESIII has collected large data samples in this energy region [33]. The cylindrical core of the BESIII detector covers 93% of the full solid angle and consists of a helium-based multilayer drift chamber (MDC), a plastic scintillator time-of-flight system (TOF), and a CsI(Tl) electromagnetic calorimeter (EMC), which are all enclosed in a superconducting solenoidal magnet providing a 1.0 T (0.9 T in 2012, for about $(1088.5 \pm 4.4) \times 10^6 J/\psi$ events [34]) magnetic field. The solenoid is supported by an octagonal flux-return yoke with resistive plate counter muon identification modules interleaved with steel. The charged-particle momentum resolution at 1 GeV/ c is 0.5%, and the specific energy deposits (dE/dx) resolution is 6% for electrons from Bhabha scattering. The EMC measures photon energies with a resolution of 2.5% (5%) at 1 GeV in the barrel (end cap) region. The time resolution in the TOF barrel region is 68 ps, while that in the end cap region is 110 ps. The end cap TOF system was upgraded in 2015 with multigap resistive plate chamber technology, providing a time resolution of 60 ps [35,36], which is used for a dataset of $(8774.0 \pm 39.4) \times 10^6 J/\psi$ events [34] taken in 2017–2019.

This analysis uses a data sample of $(10087 \pm 44) \times 10^6 J/\psi$ events [34] accumulated in e^+e^- collisions at a center-of-mass energy $\sqrt{s} = 3.097 \text{ GeV}$ by BESIII. Monte Carlo (MC) simulation of the full detector is used to determine the detection efficiency, optimize event selection criteria, and estimate backgrounds. The simulation program BOOST [37] provides an event generator, contains the detector geometry description [38], and simulates the detector response and signal digitization. The production of the J/ψ resonance is simulated by the MC event generator KKMC [39,40], while the known decay modes are generated with EvtGen [41,42] using branching fractions from the PDG [43], and the remaining unknown charmonium decays are modeled with LUNDCHARM [44,45].

For the signal MC sample, the simulation of the $J/\psi \rightarrow e^+e^-\eta(1405)$ channel takes into account the angular

distributions of the final states and the polarization of the J/ψ [46]. The subsequent decay $\eta(1405) \rightarrow \pi^0\pi^+\pi^-$ is modeled by a custom generator based on a theoretical model [21] with modifications to incorporate the TSM effects [47,48] due to the intermediate $K^*\bar{K} + \text{c.c.}$ rescatterings by exchanging an on shell kaon (antikaon) in the decay of $\eta(1405) \rightarrow \pi^0\pi^+\pi^-$. The width effect within the triangle loops and the isospin violation arising from the K^0/K^\pm mass difference within triangle loops are included. The masses of K^0 , K^\pm and the mass and width of K^{*0} are set to the world-average values [43] in the simulation.

III. EVENT SELECTION

Charged tracks detected in the MDC are required to be within a polar angle (θ) range of $|\cos \theta| < 0.93$, where θ is defined with respect to the z -axis, which is the symmetry axis of the MDC. The point of closest approach to the interaction point (IP) must have the distance to the IP less than 10 cm along the z -axis and less than 1 cm in the transverse plane. The number of good charged tracks is required to be equal to four with zero net charge. Particle identification (PID) for charged tracks combines measurements of the dE/dx in the MDC, the flight time in the TOF and the energy deposited in the EMC to form likelihoods for electron [$\mathcal{L}(e)$], pion [$\mathcal{L}(\pi)$], and kaon [$\mathcal{L}(K)$] hypotheses. Tracks are identified as electrons when the electron hypothesis has the highest PID likelihood among the three hypotheses, i.e. $\mathcal{L}(e) > \mathcal{L}(K)$ and $\mathcal{L}(e) > \mathcal{L}(\pi)$. To exclude misidentified pions, an additional $E/p > 0.8$ requirement is applied to the e^+/e^- tracks with momentum higher than 0.8 GeV/ c , where E and p are the energy deposited in the EMC and the momentum measured with the MDC, respectively. Any charged track not identified as an electron is assigned as a pion. An event is accepted if it contains exactly the track combination $e^+e^-\pi^+\pi^-$.

Photon candidates are identified using showers in the EMC. The deposited energy of each shower must be more than 25 MeV in the barrel EMC ($|\cos \theta| < 0.8$) or 50 MeV in the end cap EMC ($0.86 < |\cos \theta| < 0.92$). To exclude showers that originate from charged particles, the angle subtended by the EMC shower and the extrapolated position of the closest charged track at the EMC must be greater than 10° . To suppress electronic noise and showers unrelated to the event, the difference between the EMC time and the event start time is required to be within [0, 700] ns. At least two photons are retained in each event.

A vertex fit is performed to the four charged tracks ($e^+e^-\pi^+\pi^-$) to ensure that they originate from the same point. An energy-momentum constraint (4C) kinematic fit is also performed for the selected $J/\psi \rightarrow e^+e^-\eta(1405) \rightarrow e^+e^-\pi^0f_0(980) \rightarrow e^+e^-\pi^0\pi^+\pi^-$ candidate events. For events with more than two photon candidates, the combination with the least χ_{4C}^2 from the kinematic fit is retained. The requirement of χ_{4C}^2 is optimized based on the figure-of-merit $S/\sqrt{S+B}$, where S and B stand for the

number of signal and background events passing the above selection criteria, respectively. Finally, the χ^2_{4C} value is required to be less than 20.

A Crystal Ball function is used to describe the distribution of invariant masses of the selected photon pairs ($M_{\gamma\gamma}$). The pair is accepted as a π^0 candidate if the invariant mass $M_{\gamma\gamma}$ is within a $\pm 3\sigma$ mass window around the π^0 peak, where σ being 4.19 ± 0.02 MeV/ c^2 , is the resolution of the fitted Crystal Ball function.

The events are required to have the $\pi^+\pi^-$ invariant mass ($M_{\pi^+\pi^-}$) consistent with the world average mass of the $f_0(980)$ meson [43]. To define the $M_{\pi^+\pi^-}$ selection window, a fit to the $M_{\pi^+\pi^-}$ distribution is performed in the signal-enriched range of the $\pi^+\pi^-\pi^0$ invariant mass between 1.3 and 1.5 GeV/ c^2 [18]. The signal is described by a convolution of a Breit-Wigner function and a Gaussian resolution function while the background shape is described by a second-order Chebychev polynomial. The mass and width of the Breit-Wigner function are free parameters of the fit, while the Gaussian resolution is taken from the MC. The events with $M_{\pi^+\pi^-}$ within $\pm 3\sigma$ around the $f_0(980)$ peak are kept for the further analysis, where σ is the width of the Breit-Wigner function. The fit result is shown in Fig. 1.

Events in which a photon converts into an e^+e^- pair in the material of the detector constitute a source of background, in particular those from $J/\psi \rightarrow \gamma\eta(1405)$ decays. The distance R_{xy} from the IP to the reconstructed point of closest approach of the e^+e^- pair is used to separate the signal events from the photon-conversion background events [49]. For the signal process the e^+e^- pair comes directly from the J/ψ decay, so R_{xy} values are close to zero.

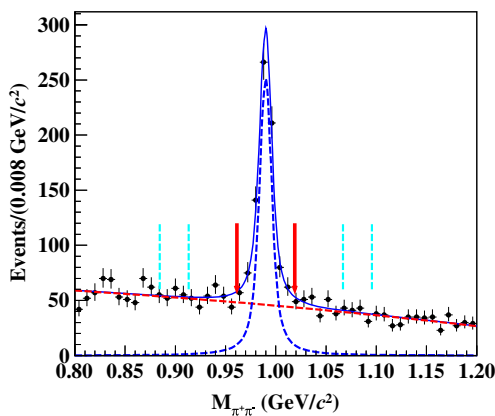


FIG. 1. Distribution of $M_{\pi^+\pi^-}$ for the accepted candidates with fit results overlaid. The dots with error bars represent data, the blue solid curve is the overall fit, the black dashed line is the fitted signal, the red dotted line represents the fitted background. The red arrows indicate the $f_0(980)$ mass window (0.961 GeV/ c^2 < $M_{\pi^+\pi^-}$ < 1.019 GeV/ c^2), and the pairs of cyan dashed vertical lines (left and right of the signal peak) indicate the $f_0(980)$ sideband regions (0.884 GeV/ c^2 < $M_{\pi^+\pi^-}$ < 0.913 GeV/ c^2 and 1.067 GeV/ c^2 < $M_{\pi^+\pi^-}$ < 1.096 GeV/ c^2).

Background events accumulate above 2 cm, where most of the photon conversions occur. To suppress this background the value of R_{xy} is required to be less than 2 cm.

Possible background contributions are studied with a sample of 2932 pb $^{-1}$ of data taken at $\sqrt{s} = 3.773$ GeV [50] and the J/ψ inclusive MC sample. The analysis of the 3.773 GeV sample indicates that the QED background is negligible, while studies of the MC sample reveal no significant sources of peaking background.

IV. BRANCHING-FRACTION MEASUREMENT

An unbinned maximum-likelihood fit is performed on the $M_{\pi^+\pi^-\pi^0}$ spectrum in the $f_0(980)$ signal and sideband regions simultaneously. After taking into account the mass dependence of the detection efficiency, the signal MC shape convoluted a Gaussian function is used as the $\eta(1405)$ signal shape. The small bump around 1.3 GeV/ c^2 is described by a Breit-Wigner function, the mass and width of which are fixed at the world-average values of the $f_1(1285)$ resonance [43]. The background is described by a Argus function with parameters determined by a simultaneous fit to the $M_{\pi^+\pi^-\pi^0}$ spectrum with $M_{\pi^+\pi^-}$ being in the $f_0(980)$ sidebands region (0.884 GeV/ c^2 < $M_{\pi^+\pi^-}$ < 0.913 GeV/ c^2 and 1.067 GeV/ c^2 < $M_{\pi^+\pi^-}$ < 1.096 GeV/ c^2). The yield of each component is a free parameter of the fit.

The fit result is shown in Fig. 2. The number of $\eta(1405)$ signal events is 203.0 ± 19.9 . The detection efficiency is estimated to be $(9.99 \pm 0.05)\%$ using the signal MC

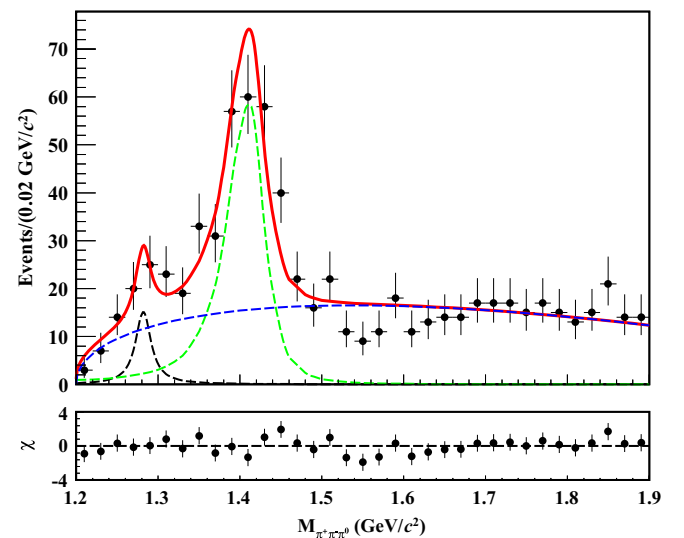


FIG. 2. Top: distribution of $M_{\pi^+\pi^-\pi^0}$ for the accepted candidates with $M_{\pi^+\pi^-}$ being in the $f_0(980)$ signal region with fit results overlaid. The black dots with error bars represent data, the red solid curve is the overall fit, the black dash-dotted line denotes the $f_1(1285)$ signal, the green dashed line denotes the $\eta(1405)$ signal and the blue dotted line is background. Bottom: the pull between the fit and data, *i.e.* the difference between data and the fit curve normalized by the uncertainty of the data in each bin.

simulation. The significance of the $\eta(1405)$ signal peak is 9.8σ , calculated from the difference of the likelihood values with and without the $\eta(1405)$ signal in the fits. The calculation of the significance takes into account the systematic effects discussed later. The measured BF of the decay $J/\psi \rightarrow e^+e^-\eta(1405) \rightarrow e^+e^-\pi^0 f_0(980) \rightarrow e^+e^-\pi^0\pi^+\pi^-$ is calculated as

$$\mathcal{B}_{\text{sig}} = \frac{N_{\text{sig}}}{N_{J/\psi} \cdot \epsilon \cdot \mathcal{B}(\pi^0 \rightarrow \gamma\gamma)}, \quad (2)$$

where N_{sig} is the number of signal events, $N_{J/\psi}$ is the total number of J/ψ events [34], ϵ is the detection efficiency and $\mathcal{B}(\pi^0 \rightarrow \gamma\gamma)$ is the BF of $\pi^0 \rightarrow \gamma\gamma$ [43]. We obtain $\mathcal{B}_{\text{sig}} = (2.04 \pm 0.20) \times 10^{-7}$ where the uncertainty is statistical only.

V. BRANCHING-FRACTION SYSTEMATIC UNCERTAINTIES

The sources of systematic uncertainties for the BF measurement include the MDC tracking efficiency, the PID efficiency, the N_{track} requirement, the photon detection efficiency, the γ conversion veto, the total number of J/ψ events, the BF of $\pi^0 \rightarrow \gamma\gamma$, the kinematic fit, the $M_{\pi^+\pi^-}$ window, the π^0 mass window, the fit range of $M_{\pi^+\pi^-\pi^0}$ and the background shape.

To study the systematic uncertainties related to the MDC tracking and PID efficiencies of e^\pm , the differences between data and MC simulation in different momentum and polar-angle regions are studied with a control sample of radiative Bhabha scattering $e^+e^- \rightarrow \gamma e^+e^-$ (including $J/\psi \rightarrow \gamma e^+e^-$) events from the same data sample. The associated systematic uncertainties are determined by applying bin-by-bin weights, which take into account the data/MC differences and the uncertainty due to the limited size of the control sample, to the momentum and polar-angle distributions of e^\pm in the signal decays. The systematic uncertainties from e^\pm tracking and PID are 0.4% and 0.5%, respectively.

The systematic uncertainty due to the $E/p > 0.8$ requirement is estimated with the same control sample and a weighting method similar to that used in the PID efficiency study. The difference in the efficiencies of the $E/p > 0.8$ requirement is tabulated in bins of high momentum and polar angle. The systematic uncertainty for the $E/p > 0.8$ requirement is determined to be 0.1%.

The systematic uncertainties from the tracking efficiency of charged pions and the photon detection efficiency are investigated by analyzing control samples of $J/\psi \rightarrow \pi^+\pi^-\pi^0$ and $e^+e^- \rightarrow \gamma\mu^+\mu^-$ events, respectively. The two-dimensional distributions of the polar angle and momentum in the signal decays are reweighted according to the observed data/MC differences and the statistical uncertainties of the control samples. The systematic

uncertainty of the π^\pm tracking efficiency is assigned to be 0.6% per track and that of photon detection efficiency is 0.5% per photon.

The control sample of $J/\psi \rightarrow \pi^+\pi^-\pi^0$, $\pi^0 \rightarrow \gamma e^+e^-$ events is used to study the systematic bias associated with the requirement of $N_{\text{track}} = 4$. The difference in the ratio of $N_{\text{track}} = 4$ to $N_{\text{track}} \geq 4$ between data and MC simulation is considered as a systematic uncertainty, which is 0.2%.

The systematic uncertainty from the photon conversion veto criterion $R_{xy} < 2$ cm is assessed with the same control sample of $J/\psi \rightarrow \pi^+\pi^-\pi^0$, $\pi^0 \rightarrow \gamma e^+e^-$ events. The relative difference of efficiencies associated with the γ conversion rejection between data and MC simulation, is 0.12%, which is taken as the associated systematic uncertainty. The MC samples of the radiation decay $J/\psi \rightarrow \gamma\eta(1405)$ are generated to estimate the systematic uncertainty from the remaining gamma conversion background in the data. Considering the selection efficiency of this MC sample and the branching fraction measured in Ref. [18], the remaining event number of this background is estimated, which is only 0.4% of the signal yields, and it is taken as the systematic uncertainty.

The track helix parameters are corrected for simulated events to reduce the difference between data and MC simulation in the χ_{4C}^2 distribution. Half of the difference in the selection efficiencies after and before the correction, 0.6%, is taken as the corresponding systematic uncertainty [51].

In the baseline fit, the resonances $f_1(1285)$ and $\eta(1405)$ are described by an incoherent sum of Breit-Wigner functions, designated as BW_1 and BW_2 , respectively. To estimate the systematic uncertainty from neglected interference effects, the probability density function (PDF) of the two resonances is constructed as

$$\text{PDF}_{\text{signal}} = (|A \times BW_1(s) + BW_2(s) \times e^{i\varphi}|^2) \otimes G(s) \times \epsilon(s), \quad (3)$$

where φ is the relative phase between the $\eta(1405)$ and $f_1(1285)$, A is the normalization factor, $G(s)$ is a Gaussian function used to describe the data-MC difference on the detector resolution, and $\epsilon(s)$ is the detection efficiency curve obtained by the MC simulation. The difference between the fits with and without interference, 1.2%, is taken to be the systematic uncertainty.

The signal region in the $M_{\pi^+\pi^-}$ distribution is widened by the width of the Breit-Wigner function that describes the distributions, and another fit is performed. The difference on the measured BF is taken as the corresponding systematic uncertainty, which is 1.5%.

The fit range of $M_{\pi^+\pi^-\pi^0}$ is changed from the baseline values $[1.2, 1.9]$ GeV/ c^2 to $[1.2, 1.84]$ GeV/ c^2 and $[1.2, 1.96]$ GeV/ c^2 and the $f_0(980)$ sideband range is changed to $(0.875 \text{ GeV}/c^2 < M_{\pi^+\pi^-} < 0.913 \text{ GeV}/c^2$

and $1.067 \text{ GeV}/c^2 < M_{\pi^+\pi^-} < 1.105 \text{ GeV}/c^2$. The largest variation on the measured BF between the alternative fits and the baseline fit, 1.5%, is assigned as the associated systematic uncertainty.

The systematic uncertainty related to the selection criterion on $M_{\gamma\gamma}$ in order to select good π^0 candidates is also considered. Differing from using a Crystal Ball function to fit the $M_{\gamma\gamma}$ distribution in data, the signal MC shape is used to perform an alternative fit to the data. The relative difference on the number of observed π^0 candidates, i.e. 1.0%, is taken as the systematic uncertainty.

The uncertainty from the TFF is estimated with the alternative signal MC samples generated with the pole mass $\Lambda = 1.80, 2.06, 2.20, 3.097$ or $3.77 \text{ GeV}/c^2$ instead of the default value $3.686 \text{ GeV}/c^2$, and the largest change of the efficiency, 1.7%, is taken as the systematic uncertainty. The uncertainty from the theoretical model is estimated as the change of the signal MC efficiency, comparing to the nominal result, when the $f_0(980)$ and $\eta(1405)$ resonances are considered as Breit-Wigner line shapes, which is 1.1%. Additionally, to determine the systematic uncertainty due to the custom generator, the known width of K^* is changed by $\pm 1\sigma$ or $\pm 2\sigma$ to produce different signal MC samples. The largest change of the efficiency, which is 0.4%, is added in quadrature to the pole mass uncertainty and theoretical model uncertainty to arrive at a total uncertainty of 2.1%, which is considered to be the systematic uncertainty associated with the signal MC generator.

The uncertainty due to the BF of $\pi^0 \rightarrow \gamma\gamma$ is 0.034% [43]. The systematic uncertainty on the total number of J/ψ events is 0.44% according to Ref. [34].

TABLE I. Relative systematic uncertainties in the branching-fraction measurement.

Source	Uncertainty (%)
e^\pm tracking	0.4
e^\pm PID	0.5
$E/p > 0.8$ requirement	0.1
π^\pm tracking	1.2
Photon detection	1.0
$N_{\text{track}} = 4$	0.2
Veto of γ conversion	0.2
γ conversion background	0.4
4C kinematic fit	0.6
Interference effects among resonances	1.2
$f_0(980)$ mass window	1.5
Fit range and background shape	1.5
π^0 mass window	1.0
Custom generator	2.1
$B(\pi^0 \rightarrow \gamma\gamma)$	<0.1
$N_{J/\psi}$	0.5
Total	3.9

All the sources of systematic uncertainties are summarized in Table I. The total systematic uncertainty is evaluated to be 3.9% from the quadratic sum of the above individual contributions.

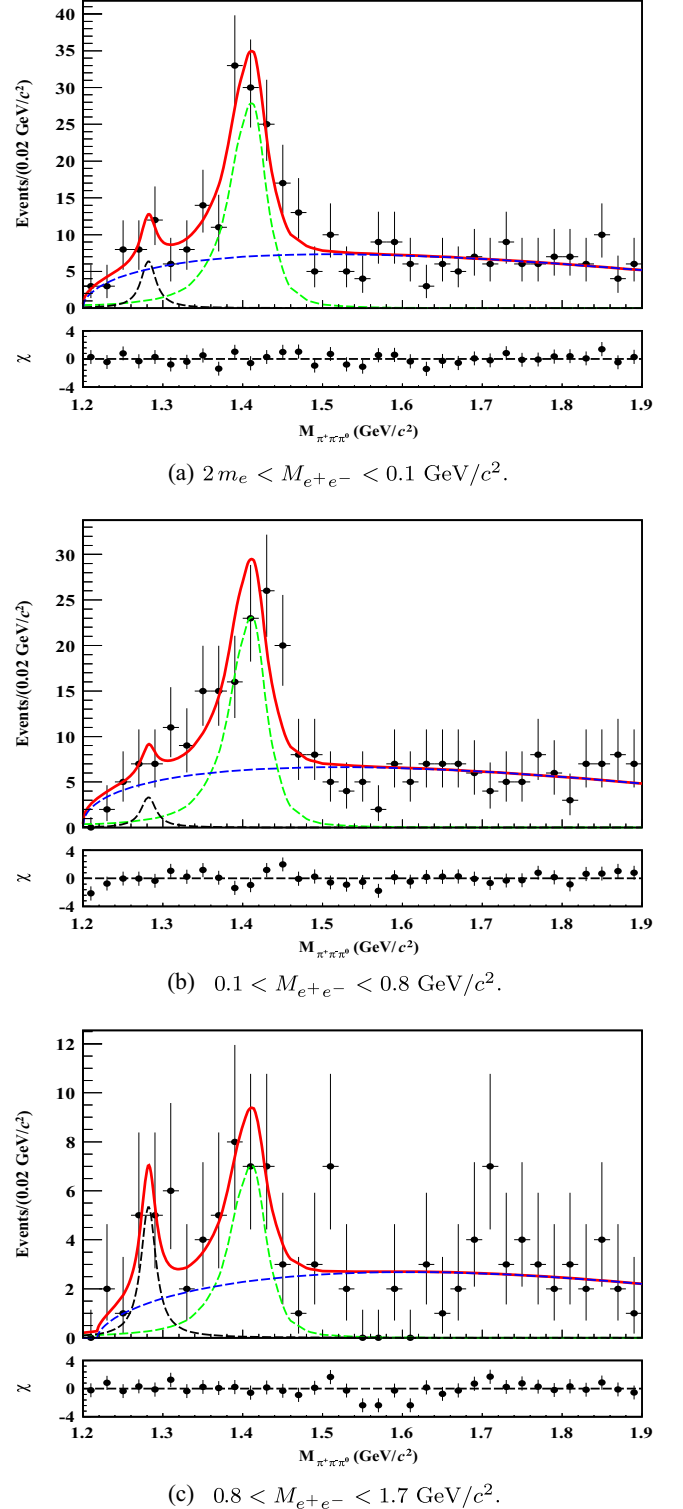


FIG. 3. The fit of $\pi^+\pi^-\pi^0$ mass spectrum for each $M_{e^+e^-}$ bin.

TABLE II. The BF ratios $\frac{\mathcal{B}(J/\psi \rightarrow e^+e^-\eta(1405))}{\mathcal{B}(J/\psi \rightarrow \gamma\eta(1405))}$ (R_{QED}) in each q^2 bin predicted by QED, the BFs of $J/\psi \rightarrow e^+e^-\eta(1405)$ predicted by QED (\mathcal{B}_{QED}), signal yields, detection efficiencies, measured branching fractions (\mathcal{B}_{fit}), $|\mathcal{F}(q^2)|^2$ values and normalized $|\mathcal{F}(q^2)|^2$ values.

q (GeV/ c^2)	R_{QED} (10^{-4})	\mathcal{B}_{QED} (10^{-8})	Signal yields	Efficiency (%)	\mathcal{B}_{fit} (10^{-8})	$ \mathcal{F}(q^2) ^2$	Normalized $ \mathcal{F}(q^2) ^2$
$[2m_e, 0.10]$	68.78	10.32 ± 0.76	96.8 ± 13.8	8.68 ± 0.05	11.19 ± 1.60	1.08 ± 0.18	1.00 ± 0.16
$[0.10, 0.80]$	29.42	4.41 ± 0.33	80.2 ± 12.8	12.32 ± 0.09	6.53 ± 1.05	1.48 ± 0.26	1.36 ± 0.24
$[0.80, 1.70]$	3.85	0.58 ± 0.04	24.4 ± 7.3	14.01 ± 0.26	1.75 ± 0.53	3.03 ± 0.95	2.80 ± 0.87

VI. TRANSITION FORM FACTOR MEASUREMENT

The TFF for $J/\psi \rightarrow e^+e^-\eta(1405)$ decay is measured by dividing the $M_{e^+e^-}$ spectrum into three intervals according to the ratio of the measured BFs and the BFs predicted by QED. The former are obtained using the same selection criteria and fit method as for the BF measurement, and the latter is calculated by integrating Eq. (12) of Ref. [29] over each bin. The fit of $\pi^+\pi^-\pi^0$ mass spectrum for each $M_{e^+e^-}$ bin are shown in Fig. 3, where the fit method is same as the one used in the BF measurement. The numerical values used to determine TFF are listed in Table II. The normalized TFF is parameterized with the usual simple pole approximation as [29]

$$\mathcal{F}(q^2) = \frac{1}{1 - q^2/\Lambda^2}, \quad (4)$$

where $q^2 = M_{e^+e^-}^2$ is the square of the invariant mass of e^+e^- pair, and the parameter Λ is the spectroscopic pole mass, which is used as a fit parameter. Figure 4 shows the result of the fit to the $M_{e^+e^-}$ dependence of $|\mathcal{F}(q^2)|^2$. From the fit, Λ is determined to be $(2.06 \pm 0.26(\text{stat}) \pm 0.07(\text{syst})) \text{ GeV}/c^2$. The systematic uncertainty on the Λ measurement is obtained by repeating the fit after considering variations similar to those used in the determination of the systematic uncertainty of the BF measurement.

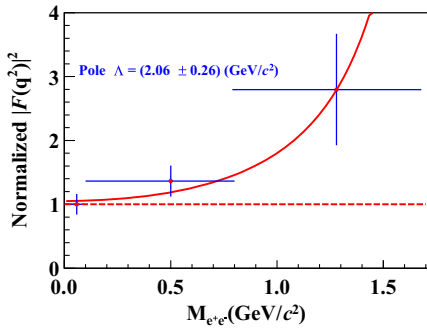


FIG. 4. The TFF distribution for the $J/\psi \rightarrow e^+e^-\eta(1405)$ decay. The dots with error bars denote the normalized $|\mathcal{F}(q^2)|^2$ values, where the horizontal error bars represent the binning width. The red solid curve is the result of the fit by the simple pole approximation, and the red dash line shows $|\mathcal{F}(q^2)|^2 = 1$.

VII. SUMMARY

Based on the data sample of $(10087 \pm 44) \times 10^6$ J/ψ events collected with the BESIII in 2009, 2012, 2018 and 2019, the EM Dalitz decay of $J/\psi \rightarrow e^+e^-\eta(1405)$ is observed for the first time via $\eta(1405) \rightarrow \pi^0 f_0(980)$ and $f_0(980) \rightarrow \pi^+\pi^-$ with a significance of 9.8σ . The BF of $J/\psi \rightarrow e^+e^-\eta(1405) \rightarrow e^+e^-\pi^0 f_0(980) \rightarrow e^+e^-\pi^0\pi^+\pi^-$ is measured to be $(2.04 \pm 0.20(\text{stat}) \pm 0.08(\text{syst})) \times 10^{-7}$, where the first uncertainty is statistical and the second one is systematic. Considering the measured BF of the radiative decay of $J/\psi \rightarrow \gamma\eta(1405) \rightarrow \gamma\pi^0 f_0(980) \rightarrow \gamma\pi^0\pi^+\pi^-$ [18], the BF ratio $\frac{\mathcal{B}(J/\psi \rightarrow e^+e^-\eta(1405))}{\mathcal{B}(J/\psi \rightarrow \gamma\eta(1405))}$ is calculated to be $(1.36 \pm 0.17(\text{stat}) \pm 0.06(\text{syst})) \times 10^{-2}$, against which future theoretical calculations can be compared. The TFF for the $J/\psi \rightarrow e^+e^-\eta(1405)$ decay is extracted by assuming the simple pole approximation. The pole value in the vector meson dominance model, $\Lambda = (2.06 \pm 0.26(\text{stat}) \pm 0.07(\text{syst})) \text{ GeV}/c^2$ is also measured. The obtained result provides valuable input for different theoretical models and understanding the intrinsic structure of $\eta(1405)$ meson.

ACKNOWLEDGMENTS

The BESIII Collaboration thanks the staff of BEPCII and the IHEP computing center for their strong support. This work is supported in part by National Key R and D Program of China under Contracts No. 2023YFA1606704, No. 2020YFA0406300, No. 2020YFA0406400; National Natural Science Foundation of China (NSFC) under Contracts No. 11805037, No. 11635010, No. 11735014, No. 11835012, No. 11935015, No. 11935016, No. 11935018, No. 11961141012, No. 12022510, No. 12025502, No. 12035009, No. 12035013, No. 12061131003, No. 12192260, No. 12192261, No. 12192262, No. 12192263, No. 12192264, No. 12192265, No. 12221005, No. 12225509, No. 12235017; the Chinese Academy of Sciences (CAS) Large-Scale Scientific Facility Program; Joint Large-Scale Scientific Facility Funds of the NSFC and CAS under Contracts No. U1832121; the CAS Center for Excellence in Particle Physics (CCEPP); CAS Key Research Program of Frontier Sciences under Contracts No. QYZDJ-SSW-SLH003, No. QYZDJ-SSW-SLH040; 100 Talents Program of CAS; The Institute of Nuclear and Particle Physics

(INPAC) and Shanghai Key Laboratory for Particle Physics and Cosmology; ERC under Contract No. 758462; European Union's Horizon 2020 research and innovation programme under Marie Skłodowska-Curie grant agreement under Contract No. 894790; German Research Foundation DFG under Contracts No. 443159800, No. 455635585, Collaborative Research Center CRC 1044, FOR5327, GRK 2149; Istituto Nazionale di Fisica Nucleare, Italy; Ministry of Development of Turkey under Contract No. DPT2006K-120470; National Research

Foundation of Korea under Contract No. NRF-2022R1A2C1092335; National Science and Technology fund of Mongolia; National Science Research and Innovation Fund (NSRF) via the Program Management Unit for Human Resources and Institutional Development, Research and Innovation of Thailand under Contract No. B16F640076; Polish National Science Centre under Contract No. 2019/35/O/ST2/02907; The Swedish Research Council; U.S. Department of Energy under Contract No. DE-FG02-05ER41374.

-
- [1] P. H. Baillon *et al.*, *Nuovo Cimento A* **50**, 393 (1967).
 [2] L. Faddeev, A. J. Niemi, and U. Wiedner, *Phys. Rev. D* **70**, 114033 (2004).
 [3] G. S. Bali, K. Schilling, A. Hulsebos, A. C. Irving, C. Michael, and P. W. Stephenson (UKQCD Collaboration), *Phys. Lett. B* **309**, 378 (1993).
 [4] C. J. Morningstar and M. J. Peardon, *Phys. Rev. D* **60**, 034509 (1999).
 [5] Y. Chen *et al.*, *Phys. Rev. D* **73**, 014516 (2006).
 [6] A. Chowdhury, A. Harindranath, and J. Maiti, *Phys. Rev. D* **91**, 074507 (2015).
 [7] M. G. Rath *et al.*, *Phys. Rev. D* **40**, 693 (1989).
 [8] Z. Bai *et al.* (Mark III Collaboration), *Phys. Rev. Lett.* **65**, 2507 (1990).
 [9] M. Acciarri *et al.* (L3 Collaboration), *Phys. Lett. B* **501**, 1 (2001).
 [10] Adams *et al.*, *Phys. Lett. B* **516**, 264 (2001).
 [11] J. E. Augustin *et al.* (DM2 Collaboration), *Phys. Rev. D* **42**, 10 (1990).
 [12] J. E. Augustin *et al.* (DM2 Collaboration), *Phys. Rev. D* **46**, 1951 (1992).
 [13] A. Bertin *et al.* (Obelix Collaboration), *Phys. Lett. B* **361**, 187 (1995).
 [14] C. Cicalò *et al.* (Obelix Collaboration), *Phys. Lett. B* **462**, 453 (1999).
 [15] A. Bertin *et al.* (Obelix Collaboration), *Phys. Lett. B* **400**, 226 (1997).
 [16] F. Nichitiu *et al.* (Obelix Collaboration), *Phys. Lett. B* **545**, 261 (2002).
 [17] E. Klempt and A. Zaitsev, *Phys. Rep.* **454**, 1 (2007).
 [18] M. Ablikim *et al.* (BESIII Collaboration), *Phys. Rev. Lett.* **108**, 182001 (2012).
 [19] J. J. Wu, X. H. Liu, Q. Zhao, and B. S. Zou, *Phys. Rev. Lett.* **108**, 081803 (2012).
 [20] X. G. Wu, J. J. Wu, Q. Zhao, and B. S. Zou, *Phys. Rev. D* **87**, 014023 (2013).
 [21] M. C. Du and Q. Zhao, *Phys. Rev. D* **100**, 036005 (2019).
 [22] M. Ablikim *et al.* (BESIII Collaboration), *Phys. Rev. D* **89**, 092008 (2014).
 [23] A. Anastasi *et al.* (KLOE-2 Collaboration), *Phys. Lett. B* **757**, 362 (2016).
 [24] P. Adlarson *et al.* (A2 Collaboration), *Phys. Rev. C* **95**, 035208 (2017).
 [25] M. Ablikim *et al.* (BESIII Collaboration), *Phys. Lett. B* **783**, 452 (2018).
 [26] F. Klingl, N. Kaiser, and W. Weise, *Z. Phys. A* **356**, 193 (1996).
 [27] A. Faessler, C. Fuchs, and M. I. Krivoruchenko, *Phys. Rev. C* **61**, 035206 (2000).
 [28] C. Terschlusen and S. Leupold, *Phys. Lett. B* **691**, 191 (2010).
 [29] L. M. Gu, H. B. Li, X. X. Ma, and M. Z. Yang, *Phys. Rev. D* **100**, 016018 (2019).
 [30] X. Jiang, F. Chen, Y. Chen, M. Gong, N. Li, Z. Liu, W. Sun, and R. Zhang, *Phys. Rev. Lett.* **130**, 061901 (2023).
 [31] M. Ablikim *et al.* (BESIII Collaboration), *Nucl. Instrum. Methods Phys. Res., Sect. A* **614**, 345 (2010).
 [32] C. H. Yu *et al.*, in *Proceedings of IPAC2016, Busan, Korea* (2016), 10.18429/JACoW-IPAC2016-TUYA01.
 [33] M. Ablikim *et al.* (BESIII Collaboration), *Chin. Phys. C* **44**, 040001 (2020).
 [34] M. Ablikim *et al.* (BESIII Collaboration), *Chin. Phys. C* **46**, 074001 (2022).
 [35] X. Li *et al.*, *Radiat. Detects Tech. Methods* **1**, 13 (2017).
 [36] Y. X. Guo *et al.*, *Radiat. Detects Tech. Methods* **1**, 15 (2017).
 [37] Z. Y. Deng *et al.*, *HEP&NP* **30**, 5 (2006) (in Chinese).
 [38] K. X. Huang *et al.*, *Nucl. Sci. Tech.* **33**, 142 (2022).
 [39] S. Jadach, B. F. L. Ward, and Z. Was, *Comput. Phys. Commun.* **130**, 260 (2000).
 [40] S. Jadach, B. F. L. Ward, and Z. Was, *Phys. Rev. D* **63**, 113009 (2001).
 [41] D. J. Lange, *Nucl. Instrum. Methods Phys. Res., Sect. A* **462**, 152 (2001).
 [42] R. G. Ping, *Chin. Phys. C* **32**, 599 (2008).
 [43] R. L. Workman *et al.* (Particle Data Group), *Prog. Theor. Exp. Phys.* **2022**, 083C01 (2022).
 [44] J. C. Chen, G. S. Huang, X. R. Qi, D. H. Zhang, and Y. S. Zhu, *Phys. Rev. D* **62**, 034003 (2000).
 [45] R. L. Yang, R. G. Ping, and H. Chen, *Chin. Phys. Lett.* **31**, 061301 (2014).

- [46] J. L. Fu, H. B. Li, X. S. Qin, and M. Z. Yang, *Mod. Phys. Lett. A* **27**, 1250223 (2012).
 [47] L. D. Landau, *Nucl. Phys.* **13**, 1 (1959).
 [48] R. E. Cutkosky, *J. Math. Phys. (N.Y.)* **1**, 429 (1960).
 [49] Z. R. Xu and K. L. He, *Chin. Phys. C* **36**, 742 (2012).
 [50] M. Ablikim *et al.* (BESIII Collaboration), *Chin. Phys. C* **37**, 123001 (2013); *Phys. Lett. B* **753**, 629 (2016).
 [51] M. Ablikim *et al.* (BESIII Collaboration), *Phys. Rev. D* **87**, 012002 (2013).

M. Ablikim,¹ M. N. Achasov,^{5,b} P. Adlarson,⁷⁵ X. C. Ai,⁸¹ R. Aliberti,³⁶ A. Amoroso,^{74a,74c} M. R. An,⁴⁰ Q. An,^{71,58} Y. Bai,⁵⁷ O. Bakina,³⁷ I. Balossino,^{30a} Y. Ban,^{47,g} V. Batozskaya,^{1,45} K. Begzsuren,³³ N. Berger,³⁶ M. Berlowski,⁴⁵ M. Bertani,^{29a} D. Bettoni,^{30a} F. Bianchi,^{74a,74c} E. Bianco,^{74a,74c} A. Bortone,^{74a,74c} I. Boyko,³⁷ R. A. Briere,⁶ A. Brueggemann,⁶⁸ H. Cai,⁷⁶ X. Cai,^{1,58} A. Calcaterra,^{29a} G. F. Cao,^{1,63} N. Cao,^{1,63} S. A. Cetin,^{62a} J. F. Chang,^{1,58} T. T. Chang,⁷⁷ W. L. Chang,^{1,63} G. R. Che,⁴⁴ G. Chelkov,^{37,a} C. Chen,⁴⁴ Chao Chen,⁵⁵ G. Chen,¹ H. S. Chen,^{1,63} M. L. Chen,^{1,58,63} S. J. Chen,⁴³ S. M. Chen,⁶¹ T. Chen,^{1,63} X. R. Chen,^{32,63} X. T. Chen,^{1,63} Y. B. Chen,^{1,58} Y. Q. Chen,³⁵ Z. J. Chen,^{26,h} W. S. Cheng,^{74c} S. K. Choi,¹¹ X. Chu,⁴⁴ G. Cibinetto,^{30a} S. C. Coen,⁴ F. Cossio,^{74c} J. J. Cui,⁵⁰ H. L. Dai,^{1,58} J. P. Dai,⁷⁹ A. Dbeyssi,¹⁹ R. E. de Boer,⁴ D. Dedovich,³⁷ Z. Y. Deng,¹ A. Denig,³⁶ I. Denysenko,³⁷ M. Destefanis,^{74a,74c} F. De Mori,^{74a,74c} B. Ding,^{66,1} X. X. Ding,^{47,g} Y. Ding,⁴¹ Y. Ding,³⁵ J. Dong,^{1,58} L. Y. Dong,^{1,63} M. Y. Dong,^{1,58,63} X. Dong,⁷⁶ M. C. Du,¹ S. X. Du,⁸¹ Z. H. Duan,⁴³ P. Egorov,^{37,a} Y. L. Fan,⁷⁶ J. Fang,^{1,58} S. S. Fang,^{1,63} W. X. Fang,¹ Y. Fang,¹ R. Farinelli,^{30a} L. Fava,^{74b,74c} F. Feldbauer,⁴ G. Felici,^{29a} C. Q. Feng,^{71,58} J. H. Feng,⁵⁹ K. Fischer,⁶⁹ M. Fritsch,⁴ C. Fritsch,⁶⁸ C. D. Fu,¹ J. L. Fu,⁶³ Y. W. Fu,¹ H. Gao,⁶³ Y. N. Gao,^{47,g} Yang Gao,^{71,58} S. Garbolino,^{74c} I. Garzia,^{30a,30b} P. T. Ge,⁷⁶ Z. W. Ge,⁴³ C. Geng,⁵⁹ E. M. Gersabeck,⁶⁷ A. Gilman,⁶⁹ K. Goetzen,¹⁴ L. Gong,⁴¹ W. X. Gong,^{1,58} W. Gradl,³⁶ S. Gramigna,^{30a,30b} M. Greco,^{74a,74c} M. H. Gu,^{1,58} Y. T. Gu,¹⁶ C. Y. Guan,^{1,63} Z. L. Guan,²³ A. Q. Guo,^{32,63} L. B. Guo,⁴² M. J. Guo,⁵⁰ R. P. Guo,⁴⁹ Y. P. Guo,^{13,f} A. Guskov,^{37,a} T. T. Han,⁵⁰ W. Y. Han,⁴⁰ X. Q. Hao,²⁰ F. A. Harris,⁶⁵ K. K. He,⁵⁵ K. L. He,^{1,63} F. H. H. Heinsius,⁴ C. H. Heinz,³⁶ Y. K. Heng,^{1,58,63} C. Herold,⁶⁰ T. Holtmann,⁴ P. C. Hong,^{13,f} G. Y. Hou,^{1,63} X. T. Hou,^{1,63} Y. R. Hou,⁶³ Z. L. Hou,¹ H. M. Hu,^{1,63} J. F. Hu,^{56,i} T. Hu,^{1,58,63} Y. Hu,¹ G. S. Huang,^{71,58} K. X. Huang,⁵⁹ L. Q. Huang,^{32,63} X. T. Huang,⁵⁰ Y. P. Huang,¹ T. Hussain,⁷³ N. Hüsken,^{28,36} W. Imoehl,²⁸ M. Irshad,^{71,58} J. Jackson,²⁸ S. Jaeger,⁴ S. Janchiv,³³ J. H. Jeong,¹¹ Q. Ji,¹ Q. P. Ji,²⁰ X. B. Ji,^{1,63} X. L. Ji,^{1,58} Y. Y. Ji,⁵⁰ X. Q. Jia,⁵⁰ Z. K. Jia,^{71,58} H. J. Jiang,⁷⁶ P. C. Jiang,^{47,g} S. S. Jiang,⁴⁰ T. J. Jiang,¹⁷ X. S. Jiang,^{1,58,63} Y. Jiang,⁶³ J. B. Jiao,⁵⁰ Z. Jiao,²⁴ S. Jin,⁴³ Y. Jin,⁶⁶ M. Q. Jing,^{1,63} T. Johansson,⁷⁵ X. Kui,¹ S. Kabana,³⁴ N. Kalantar-Nayestanaki,⁶⁴ X. L. Kang,¹⁰ X. S. Kang,⁴¹ R. Kappert,⁶⁴ M. Kavatsyuk,⁶⁴ B. C. Ke,⁸¹ A. Khoukaz,⁶⁸ R. Kiuchi,¹ R. Kliemt,¹⁴ O. B. Kolcu,^{62a} B. Kopf,⁴ M. K. Kuessner,⁴ A. Kupsc,^{45,75} W. Kühn,³⁸ J. J. Lane,⁶⁷ P. Larin,¹⁹ A. Lavania,²⁷ L. Lavezzi,^{74a,74c} T. T. Lei,^{71,k} Z. H. Lei,^{71,58} H. Leithoff,³⁶ M. Lellmann,³⁶ T. Lenz,³⁶ C. Li,⁴⁴ C. Li,⁴⁸ C. H. Li,⁴⁰ Cheng Li,^{71,58} D. M. Li,⁸¹ F. Li,^{1,58} G. Li,¹ H. Li,^{71,58} H. B. Li,^{1,63} H. J. Li,²⁰ H. N. Li,^{56,i} Hui Li,⁴⁴ J. R. Li,⁶¹ J. S. Li,⁵⁹ J. W. Li,⁵⁰ K. L. Li,²⁰ Ke Li,¹ L. J. Li,^{1,63} L. K. Li,¹ Lei Li,³ M. H. Li,⁴⁴ P. R. Li,^{39,j,k} Q. X. Li,⁵⁰ S. X. Li,¹³ T. Li,⁵⁰ W. D. Li,^{1,63} W. G. Li,¹ X. H. Li,^{71,58} X. L. Li,⁵⁰ Xiaoyu Li,^{1,63} Y. G. Li,^{47,g} Z. J. Li,⁵⁹ Z. X. Li,¹⁶ C. Liang,⁴³ H. Liang,³⁵ H. Liang,^{1,63} H. Liang,^{71,58} Y. F. Liang,⁵⁴ Y. T. Liang,^{32,63} G. R. Liao,¹⁵ L. Z. Liao,⁵⁰ Y. P. Liao,^{1,63} J. Libby,²⁷ A. Limphirat,⁶⁰ D. X. Lin,^{32,63} T. Lin,¹ B. J. Liu,¹ B. X. Liu,⁷⁶ C. Liu,³⁵ C. X. Liu,¹ F. H. Liu,⁵³ Fang Liu,¹ Feng Liu,⁷ G. M. Liu,^{56,i} H. Liu,^{39,j,k} H. B. Liu,¹⁶ H. M. Liu,^{1,63} Huanhuan Liu,¹ Huihui Liu,²² J. B. Liu,^{71,58} J. L. Liu,⁷² J. Y. Liu,^{1,63} K. Liu,¹ K. Y. Liu,⁴¹ Ke Liu,²³ L. Liu,^{71,58} L. C. Liu,⁴⁴ Lu Liu,⁴⁴ M. H. Liu,^{13,f} P. L. Liu,¹ Q. Liu,⁶³ S. B. Liu,^{71,58} T. Liu,^{13,f} W. K. Liu,⁴⁴ W. M. Liu,^{71,58} X. Liu,^{39,j,k} Y. Liu,^{39,j,k} Y. Liu,⁸¹ Y. B. Liu,⁴⁴ Z. A. Liu,^{1,58,63} Z. Q. Liu,⁵⁰ X. C. Lou,^{1,58,63} F. X. Lu,⁵⁹ H. J. Lu,²⁴ J. G. Lu,^{1,58} X. L. Lu,¹ Y. Lu,⁸ Y. P. Lu,^{1,58} Z. H. Lu,^{1,63} C. L. Luo,⁴² M. X. Luo,⁸⁰ T. Luo,^{13,f} X. L. Luo,^{1,58} X. R. Lyu,⁶³ Y. F. Lyu,⁴⁴ F. C. Ma,⁴¹ H. L. Ma,¹ J. L. Ma,^{1,63} L. L. Ma,⁵⁰ M. M. Ma,^{1,63} Q. M. Ma,¹ R. Q. Ma,^{1,63} R. T. Ma,⁶³ X. Y. Ma,^{1,58} Y. Ma,^{47,g} Y. M. Ma,³² F. E. Maas,¹⁹ M. Maggiora,^{74a,74c} S. Malde,⁶⁹ Q. A. Malik,⁷³ A. Mangoni,^{29b} Y. J. Mao,^{47,g} Z. P. Mao,¹ S. Marcello,^{74a,74c} Z. X. Meng,⁶⁶ J. G. Messchendorp,^{14,64} G. Mezzadri,^{30a} H. Miao,^{1,63} T. J. Min,⁴³ R. E. Mitchell,²⁸ X. H. Mo,^{1,58,63} N. Yu. Muchnoi,^{5,b} Y. Nefedov,³⁷ F. Nerling,^{19,d} I. B. Nikolaev,^{5,b} Z. Ning,^{1,58} S. Nisar,^{12,l} Y. Niu,⁵⁰ S. L. Olsen,⁶³ Q. Ouyang,^{1,58,63} S. Pacetti,^{29b,29c} X. Pan,⁵⁵ Y. Pan,⁵⁷ A. Pathak,³⁵ P. Patteri,^{29a} Y. P. Pei,^{71,58} M. Pelizaeus,⁴ H. P. Peng,^{71,58} K. Peters,^{14,d} J. L. Ping,⁴² R. G. Ping,^{1,63} S. Plura,³⁶ S. Pogodin,³⁷ V. Prasad,³⁴ F. Z. Qi,¹ H. Qi,^{71,58} H. R. Qi,⁶¹ M. Qi,⁴³ T. Y. Qi,^{13,f} S. Qian,^{1,58} W. B. Qian,⁶³ C. F. Qiao,⁶³ J. J. Qin,⁷² L. Q. Qin,¹⁵ X. P. Qin,^{13,f} X. S. Qin,⁵⁰ Z. H. Qin,^{1,58} J. F. Qiu,¹ S. Q. Qu,⁶¹ C. F. Redmer,³⁶ K. J. Ren,⁴⁰ A. Rivetti,^{74c} V. Rodin,⁶⁴ M. Rolo,^{74c} G. Rong,^{1,63} Ch. Rosner,¹⁹ S. N. Ruan,⁴⁴ N. Salone,⁴⁵ A. Sarantsev,^{37,c} Y. Schelhaas,³⁶ K. Schoenning,⁷⁵ M. Scodreggio,^{30a,30b} K. Y. Shan,^{13,f} W. Shan,²⁵ X. Y. Shan,^{71,58} J. F. Shangguan,⁵⁵ L. G. Shao,^{1,63}

M. Shao,^{71,58} C. P. Shen,^{13,f} H. F. Shen,^{1,63} W. H. Shen,⁶³ X. Y. Shen,^{1,63} B. A. Shi,⁶³ H. C. Shi,^{71,58} J. L. Shi,¹³ J. Y. Shi,¹ Q. Q. Shi,⁵⁵ R. S. Shi,^{1,63} X. Shi,^{1,58} J. J. Song,²⁰ T. Z. Song,⁵⁹ W. M. Song,^{35,1} Y. J. Song,¹³ Y. X. Song,^{47,g} S. Sosio,^{74a,74c} S. Spataro,^{74a,74c} F. Stieler,³⁶ Y. J. Su,⁶³ G. B. Sun,⁷⁶ G. X. Sun,¹ H. Sun,⁶³ H. K. Sun,¹ J. F. Sun,²⁰ K. Sun,⁶¹ L. Sun,⁷⁶ S. S. Sun,^{1,63} T. Sun,^{1,63} W. Y. Sun,³⁵ Y. Sun,¹⁰ Y. J. Sun,^{71,58} Y. Z. Sun,¹ Z. T. Sun,⁵⁰ Y. X. Tan,^{71,58} C. J. Tang,⁵⁴ G. Y. Tang,¹ J. Tang,⁵⁹ Y. A. Tang,⁷⁶ L. Y. Tao,⁷² Q. T. Tao,^{26,h} M. Tat,⁶⁹ J. X. Teng,^{71,58} V. Thoren,⁷⁵ W. H. Tian,⁵⁹ W. H. Tian,⁵² Y. Tian,^{32,63} Z. F. Tian,⁷⁶ I. Uman,^{62b} S. J. Wang,⁵⁰ B. Wang,¹ B. L. Wang,⁶³ Bo Wang,^{71,58} C. W. Wang,⁴³ D. Y. Wang,^{47,g} F. Wang,⁷² H. J. Wang,^{39,j,k} H. P. Wang,^{1,63} J. P. Wang,⁵⁰ K. Wang,^{1,58} L. L. Wang,¹ M. Wang,⁵⁰ Meng Wang,^{1,63} S. Wang,^{39,j,k} S. Wang,^{13,f} T. Wang,^{13,f} T. J. Wang,⁴⁴ W. Wang,⁷² W. Wang,⁵⁹ W. P. Wang,^{71,58} X. Wang,^{47,g} X. F. Wang,^{39,j,k} X. J. Wang,⁴⁰ X. L. Wang,^{13,f} Y. Wang,⁶¹ Y. D. Wang,⁴⁶ Y. F. Wang,^{1,58,63} Y. H. Wang,⁴⁸ Y. N. Wang,⁴⁶ Y. Q. Wang,¹ Yaqian Wang,^{18,1} Yi Wang,⁶¹ Z. Wang,^{1,58} Z. L. Wang,⁷² Z. Y. Wang,^{1,63} Ziyi Wang,⁶³ D. Wei,⁷⁰ D. H. Wei,¹⁵ F. Weidner,⁶⁸ S. P. Wen,¹ C. W. Wenzel,⁴ U. W. Wiedner,⁴ G. Wilkinson,⁶⁹ M. Wolke,⁷⁵ L. Wollenberg,⁴ C. Wu,⁴⁰ J. F. Wu,^{1,63} L. H. Wu,¹ L. J. Wu,^{1,63} X. Wu,^{13,f} X. H. Wu,³⁵ Y. Wu,⁷¹ Y. J. Wu,³² Z. Wu,^{1,58} L. Xia,^{71,58} X. M. Xian,⁴⁰ T. Xiang,^{47,g} D. Xiao,^{39,j,k} G. Y. Xiao,⁴³ H. Xiao,^{13,f} S. Y. Xiao,¹ Y. L. Xiao,^{13,f} Z. J. Xiao,⁴² C. Xie,⁴³ X. H. Xie,^{47,g} Y. Xie,⁵⁰ Y. G. Xie,^{1,58} Y. H. Xie,⁷ Z. P. Xie,^{71,58} T. Y. Xing,^{1,63} C. F. Xu,^{1,63} C. J. Xu,⁵⁹ G. F. Xu,¹ H. Y. Xu,⁶⁶ Q. J. Xu,¹⁷ Q. N. Xu,³¹ W. Xu,^{1,63} W. L. Xu,⁶⁶ X. P. Xu,⁵⁵ Y. C. Xu,⁷⁸ Z. P. Xu,⁴³ Z. S. Xu,⁶³ F. Yan,^{13,f} L. Yan,^{13,f} W. B. Yan,^{71,58} W. C. Yan,⁸¹ X. Q. Yan,¹ H. J. Yang,^{51,e} H. L. Yang,³⁵ H. X. Yang,¹ Tao Yang,¹ Y. Yang,^{13,f} Y. F. Yang,⁴⁴ Y. X. Yang,^{1,63} Yifan Yang,^{1,63} Z. W. Yang,^{39,j,k} Z. P. Yao,⁵⁰ M. Ye,^{1,58} M. H. Ye,⁹ J. H. Yin,¹ Z. Y. You,⁵⁹ B. X. Yu,^{1,58,63} C. X. Yu,⁴⁴ G. Yu,^{1,63} J. S. Yu,^{26,h} T. Yu,⁷² X. D. Yu,^{47,g} C. Z. Yuan,^{1,63} L. Yuan,² S. C. Yuan,¹ X. Q. Yuan,¹ Y. Yuan,^{1,63} Z. Y. Yuan,⁵⁹ C. X. Yue,⁴⁰ A. A. Zafar,⁷³ F. R. Zeng,⁵⁰ X. Zeng,^{13,f} Y. Zeng,^{26,h} Y. J. Zeng,^{1,63} X. Y. Zhai,³⁵ Y. C. Zhai,⁵⁰ Y. H. Zhan,⁵⁹ A. Q. Zhang,^{1,63} B. L. Zhang,^{1,63} B. X. Zhang,¹ D. H. Zhang,⁴⁴ G. Y. Zhang,²⁰ H. Zhang,⁷¹ H. H. Zhang,⁵⁹ H. H. Zhang,³⁵ H. Q. Zhang,^{1,58,63} H. Y. Zhang,^{1,58} J. J. Zhang,⁵² J. L. Zhang,²¹ J. Q. Zhang,⁴² J. W. Zhang,^{1,58,63} J. X. Zhang,^{39,j,k} J. Y. Zhang,¹ J. Z. Zhang,^{1,63} Jianyu Zhang,⁶³ Jiawei Zhang,^{1,63} L. M. Zhang,⁶¹ L. Q. Zhang,⁵⁹ Lei Zhang,⁴³ P. Zhang,¹ Q. Y. Zhang,^{40,81} Shuihan Zhang,^{1,63} Shulei Zhang,^{26,h} X. D. Zhang,⁴⁶ X. M. Zhang,¹ X. Y. Zhang,⁵⁰ Xuyan Zhang,⁵⁵ Y. Zhang,⁷² Y. Zhang,⁶⁹ Y. T. Zhang,⁸¹ Y. H. Zhang,^{1,58} Yan Zhang,^{71,58} Yao Zhang,¹ Z. H. Zhang,¹ Z. L. Zhang,³⁵ Z. Y. Zhang,⁴⁴ Z. Y. Zhang,⁷⁶ G. Zhao,¹ J. Zhao,⁴⁰ J. Y. Zhao,^{1,63} J. Z. Zhao,^{1,58} Lei Zhao,^{71,58} Ling Zhao,¹ M. G. Zhao,⁴⁴ S. J. Zhao,⁸¹ Y. B. Zhao,^{1,58} Y. X. Zhao,^{32,63} Z. G. Zhao,^{71,58} A. Zhemchugov,^{37,a} B. Zheng,⁷² J. P. Zheng,^{1,58} W. J. Zheng,^{1,63} Y. H. Zheng,⁶³ B. Zhong,⁴² X. Zhong,⁵⁹ H. Zhou,⁵⁰ L. P. Zhou,^{1,63} X. Zhou,⁷⁶ X. K. Zhou,⁷ X. R. Zhou,^{71,58} X. Y. Zhou,⁴⁰ Y. Z. Zhou,^{13,f} J. Zhu,⁴⁴ K. Zhu,¹ K. J. Zhu,^{1,58,63} L. Zhu,³⁵ L. X. Zhu,⁶³ S. H. Zhu,⁷⁰ S. Q. Zhu,⁴³ T. J. Zhu,^{13,f} W. J. Zhu,^{13,f} Y. C. Zhu,^{71,58} Z. A. Zhu,^{1,63} J. H. Zou,¹ and J. Zu^{71,58}

(BESIII Collaboration)

¹*Institute of High Energy Physics, Beijing 100049, People's Republic of China*²*Beihang University, Beijing 100191, People's Republic of China*³*Beijing Institute of Petrochemical Technology, Beijing 102617, People's Republic of China*⁴*Bochum Ruhr-University, D-44780 Bochum, Germany*⁵*Budker Institute of Nuclear Physics SB RAS (BINP), Novosibirsk 630090, Russia*⁶*Carnegie Mellon University, Pittsburgh, Pennsylvania 15213, USA*⁷*Central China Normal University, Wuhan 430079, People's Republic of China*⁸*Central South University, Changsha 410083, People's Republic of China*⁹*China Center of Advanced Science and Technology, Beijing 100190, People's Republic of China*¹⁰*China University of Geosciences, Wuhan 430074, People's Republic of China*¹¹*Chung-Ang University, Seoul, 06974, Republic of Korea*¹²*COMSATS University Islamabad, Lahore Campus, Defence Road, Off Raiwind Road, 54000 Lahore, Pakistan*¹³*Fudan University, Shanghai 200433, People's Republic of China*¹⁴*GSI Helmholtzcentre for Heavy Ion Research GmbH, D-64291 Darmstadt, Germany*¹⁵*Guangxi Normal University, Guilin 541004, People's Republic of China*¹⁶*Guangxi University, Nanning 530004, People's Republic of China*¹⁷*Hangzhou Normal University, Hangzhou 310036, People's Republic of China*¹⁸*Hebei University, Baoding 071002, People's Republic of China*¹⁹*Helmholtz Institute Mainz, Staudinger Weg 18, D-55099 Mainz, Germany*²⁰*Henan Normal University, Xinxiang 453007, People's Republic of China*

- ²¹*Henan University, Kaifeng 475004, People's Republic of China*
- ²²*Henan University of Science and Technology, Luoyang 471003, People's Republic of China*
- ²³*Henan University of Technology, Zhengzhou 450001, People's Republic of China*
- ²⁴*Huangshan College, Huangshan 245000, People's Republic of China*
- ²⁵*Hunan Normal University, Changsha 410081, People's Republic of China*
- ²⁶*Hunan University, Changsha 410082, People's Republic of China*
- ²⁷*Indian Institute of Technology Madras, Chennai 600036, India*
- ²⁸*Indiana University, Bloomington, Indiana 47405, USA*
- ^{29a}*INFN Laboratori Nazionali di Frascati, I-00044, Frascati, Italy*
- ^{29b}*INFN Sezione di Perugia, I-06100, Perugia, Italy*
- ^{29c}*University of Perugia, I-06100, Perugia, Italy*
- ^{30a}*INFN Sezione di Ferrara, I-44122, Ferrara, Italy*
- ^{30b}*University of Ferrara, I-44122, Ferrara, Italy*
- ³¹*Inner Mongolia University, Hohhot 010021, People's Republic of China*
- ³²*Institute of Modern Physics, Lanzhou 730000, People's Republic of China*
- ³³*Institute of Physics and Technology, Peace Avenue 54B, Ulaanbaatar 13330, Mongolia*
- ³⁴*Instituto de Alta Investigación, Universidad de Tarapacá, Casilla 7D, Arica 1000000, Chile*
- ³⁵*Jilin University, Changchun 130012, People's Republic of China*
- ³⁶*Johannes Gutenberg University of Mainz, Johann-Joachim-Becher-Weg 45, D-55099 Mainz, Germany*
- ³⁷*Joint Institute for Nuclear Research, 141980 Dubna, Moscow region, Russia*
- ³⁸*Justus-Liebig-Universitaet Giessen, II. Physikalisches Institut, Heinrich-Buff-Ring 16, D-35392 Giessen, Germany*
- ³⁹*Lanzhou University, Lanzhou 730000, People's Republic of China*
- ⁴⁰*Liaoning Normal University, Dalian 116029, People's Republic of China*
- ⁴¹*Liaoning University, Shenyang 110036, People's Republic of China*
- ⁴²*Nanjing Normal University, Nanjing 210023, People's Republic of China*
- ⁴³*Nanjing University, Nanjing 210093, People's Republic of China*
- ⁴⁴*Nankai University, Tianjin 300071, People's Republic of China*
- ⁴⁵*National Centre for Nuclear Research, Warsaw 02-093, Poland*
- ⁴⁶*North China Electric Power University, Beijing 102206, People's Republic of China*
- ⁴⁷*Peking University, Beijing 100871, People's Republic of China*
- ⁴⁸*Qufu Normal University, Qufu 273165, People's Republic of China*
- ⁴⁹*Shandong Normal University, Jinan 250014, People's Republic of China*
- ⁵⁰*Shandong University, Jinan 250100, People's Republic of China*
- ⁵¹*Shanghai Jiao Tong University, Shanghai 200240, People's Republic of China*
- ⁵²*Shanxi Normal University, Linfen 041004, People's Republic of China*
- ⁵³*Shanxi University, Taiyuan 030006, People's Republic of China*
- ⁵⁴*Sichuan University, Chengdu 610064, People's Republic of China*
- ⁵⁵*Soochow University, Suzhou 215006, People's Republic of China*
- ⁵⁶*South China Normal University, Guangzhou 510006, People's Republic of China*
- ⁵⁷*Southeast University, Nanjing 211100, People's Republic of China*
- ⁵⁸*State Key Laboratory of Particle Detection and Electronics, Beijing 100049, Hefei 230026, People's Republic of China*
- ⁵⁹*Sun Yat-Sen University, Guangzhou 510275, People's Republic of China*
- ⁶⁰*Suranaree University of Technology, University Avenue 111, Nakhon Ratchasima 30000, Thailand*
- ⁶¹*Tsinghua University, Beijing 100084, People's Republic of China*
- ^{62a}*Turkish Accelerator Center Particle Factory Group, Istinye University, 34010, Istanbul, Turkey*
- ^{62b}*Near East University, Nicosia, North Cyprus, 99138, Mersin 10, Turkey*
- ⁶³*University of Chinese Academy of Sciences, Beijing 100049, People's Republic of China*
- ⁶⁴*University of Groningen, NL-9747 AA Groningen, The Netherlands*
- ⁶⁵*University of Hawaii, Honolulu, Hawaii 96822, USA*
- ⁶⁶*University of Jinan, Jinan 250022, People's Republic of China*
- ⁶⁷*University of Manchester, Oxford Road, Manchester, M13 9PL, United Kingdom*
- ⁶⁸*University of Muenster, Wilhelm-Klemm-Strasse 9, 48149 Muenster, Germany*
- ⁶⁹*University of Oxford, Keble Road, Oxford OX13RH, United Kingdom*
- ⁷⁰*University of Science and Technology Liaoning, Anshan 114051, People's Republic of China*
- ⁷¹*University of Science and Technology of China, Hefei 230026, People's Republic of China*
- ⁷²*University of South China, Hengyang 421001, People's Republic of China*
- ⁷³*University of the Punjab, Lahore-54590, Pakistan*
- ^{74a}*University of Turin, I-10125, Turin, Italy*

^{74b}*University of Eastern Piedmont, I-15121, Alessandria, Italy*

^{74c}*INFN, I-10125, Turin, Italy*

⁷⁵*Uppsala University, Box 516, SE-75120 Uppsala, Sweden*

⁷⁶*Wuhan University, Wuhan 430072, People's Republic of China*

⁷⁷*Xinyang Normal University, Xinyang 464000, People's Republic of China*

⁷⁸*Yantai University, Yantai 264005, People's Republic of China*

⁷⁹*Yunnan University, Kunming 650500, People's Republic of China*

⁸⁰*Zhejiang University, Hangzhou 310027, People's Republic of China*

⁸¹*Zhengzhou University, Zhengzhou 450001, People's Republic of China*

^aAlso at the Moscow Institute of Physics and Technology, Moscow 141700, Russia.

^bAlso at the Novosibirsk State University, Novosibirsk, 630090, Russia.

^cAlso at the NRC "Kurchatov Institute," PNPI, 188300, Gatchina, Russia.

^dAlso at Goethe University Frankfurt, 60323 Frankfurt am Main, Germany.

^eAlso at Key Laboratory for Particle Physics, Astrophysics and Cosmology, Ministry of Education; Shanghai Key Laboratory for Particle Physics and Cosmology; Institute of Nuclear and Particle Physics, Shanghai 200240, People's Republic of China.

^fAlso at Key Laboratory of Nuclear Physics and Ion-beam Application (MOE) and Institute of Modern Physics, Fudan University, Shanghai 200443, People's Republic of China.

^gAlso at State Key Laboratory of Nuclear Physics and Technology, Peking University, Beijing 100871, People's Republic of China.

^hAlso at School of Physics and Electronics, Hunan University, Changsha 410082, China.

ⁱAlso at Guangdong Provincial Key Laboratory of Nuclear Science, Institute of Quantum Matter, South China Normal University, Guangzhou 510006, China.

^jAlso at Frontiers Science Center for Rare Isotopes, Lanzhou University, Lanzhou 730000, People's Republic of China.

^kAlso at Lanzhou Center for Theoretical Physics, Lanzhou University, Lanzhou 730000, People's Republic of China.

^lAlso at the Department of Mathematical Sciences, IBA, Karachi 75270, Pakistan.